RESEARCH PAPER

Radon mapping in Piedmont (North-West Italy): a radio-geo-lithological approach

Enrico Chiaberto[1], Paolo Falletti[2] and Mauro Magnoni[1]*

[1]ARPA Piemonte – Department of Physical and Technological Risks, Via Guglielmo Jervis, Ivrea, Italy; [2]ARPA Piemonte – Department of Natural and Environmental Risks, Via Felice Piacenza, Biella, Italy

Abstract

***Background*:** In this work a radon mapping method implemented in Piedmont, an Italian Region in the Northern part of the country, is presented and discussed.
***Methods*:** The method is based on a "mixed approach", combining together an experimental approach, based on a large set of experimental radon measurements performed with nuclear track detectors, and an empirical model, based on the geo-lithological characteristics of soils and rocks. This approach was named as "radio-geo-lithological" because the identification of geo-lithological units was defined considering not only the usual geological classification of the territory but also the radioactivity content of the most widespread rocks and soils of Piedmont.
***Results and Conclusion*:** This method allowed to classification of all municipalities of Piedmont (1181), thus permitting the identification of the Radon Priority Areas, a provision required by the new Italian law (Legislative Decree 101/2020), implementing the European *Basic Safety Standards* (Euratom Directive 59/2013).

Keywords: *radon mapping*; *log-normal distributions*; *radio-geo-lithological units*; *radio-geo-litological model*; *priority areas*

Introduction

In spite of the well-known radon spatial and temporal variability, radon mapping is still a very useful tool for the implementation of effective and efficient radon action plans. Although a radon map cannot be used to predict the radon level in a single dwelling, it can be, nevertheless, very useful, in particular, for the prioritization of the measures to be adopted in certain areas, in order to reduce the population exposure. This fact was clearly recognized also in recent laws and regulations. In particular, the Directive 59/2013 Euratom (1) mentions explicitly radon mapping as a technical instrument for the definition of the radon priority areas (RPAs), the former *radon prone areas*, defined as the areas of a given territory (State or Region) where the probability of occurrence of high indoor radon concentrations is significantly greater than other parts of the country.

The first indoor radon campaign in Piedmont (North-West Italy) dates back to the nineties of the previous century (1990–1991): it was a regional survey involving about 450 dwellings and started as part of the Italian National Radon Survey (1989–1994) (2–6). This survey, principally aimed to give an estimate of the average exposure to radon of the Italian population, was carried out on a regional basis, involving the 21 administrative districts (Regions and Autonome Provinces) in which Italy is subdivided (Fig. 1a). The experimental work was performed by local laboratories, equipped with the same instrumentation and following same measurement protocols.

A stratified sampling scheme was used, considering all the towns above 100,000 inhabitants (50) and 150 towns/villages under 100,000 inhabitants randomly chosen, giving a total of 39 strata. In each stratum, the dwellings were randomly sampled. The survey was, thus, also able to give a first characterization of the indoor radon spatial distribution pattern in Italy, although limited to a regional level (Fig. 1b): the national mean value was found to be 70 Bq/m^3, and the regional averages ranging from 25 to 125 Bq/m^3. In Piedmont, the estimated mean value was almost identical of the national one: 69 Bq/m^3.

However, due to the intrinsic structural characteristics of the survey, very important local details were obviously completely missed. At the beginning of 2000, the knowledge of the radon distribution in Piedmont either in dwellings or workplaces was in fact very poor: after the well-designed but limited National Survey, only very few indoor radon measurements were performed, involving, in particular, little villages and towns where radon was supposed to be present in anomalous concentrations due to geological characteristics (7).

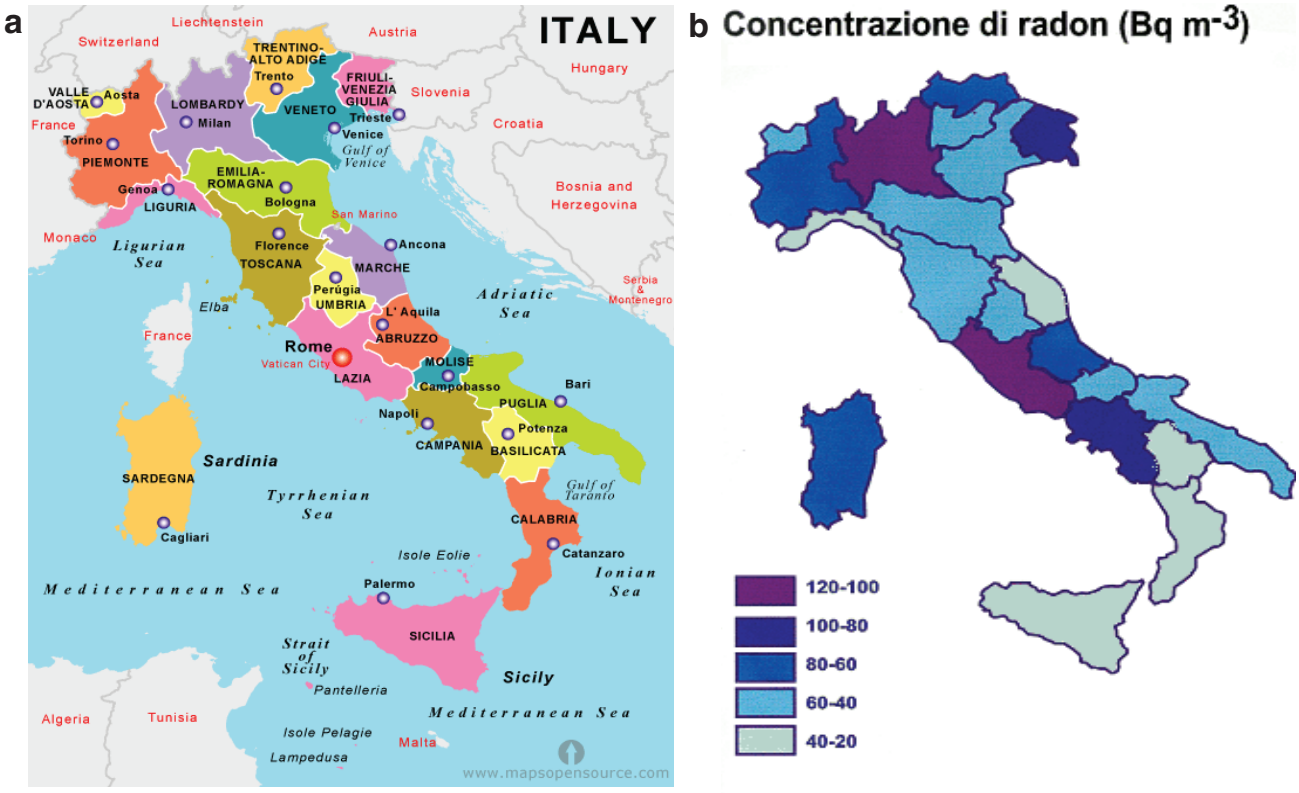

Fig. 1. (a) Italy's regional administrative subdivision and (b) the corresponding indoor radon regional averages according to the Italian National Survey (1989–1994).

For that reason, in 2007, the local government of Piedmont promoted and financed a study, assigned to ARPA Piemonte, aiming to produce a more detailed regional map of indoor radon, in compliance with the provisions established by the law. A new monitoring program was then set up in order to obtain a quite detailed picture of the distribution of the radon indoor activity concentration through the Region (8, 9). More recently, the Legislative Decree n°101/2020 (10) was implemented in the Italian legislation the Directive 59/2013 Euratom, further emphasizing the need of a regional radon map: the article 11 of the Decree establishes that the Regions have to identify the RPAs according to specific technical criteria. In particular, the RPAs are defined as portions of territory of a given Region where the percentage of building $P_{>RL}$, in which the radon activity concentration is greater than the Reference Level RL = 300 Bq/m^3, exceeds 15% of the total. Therefore, in order to fulfill this task, the ARPA Piemonte has promoted a comprehensive study, aiming to map the Region allowing the estimation for all of the 1,181 municipalities in which Piedmont is subdivided, which has the following expression:

$$P_{>RL} = 100 \times \int_{RL}^{\infty} f(C)\,dc \qquad (1)$$

in which the function $f(C)$ is the probability density function of the radon activity concentrations, assumed to be log-normal.

Thus, the mapping strategy should be designed to reach this goal, that is, the evaluation of the function $f(C)$ for each municipality. However, as the m and s parameters characterizing the log-normal distributions of the probability density functions of each sample unit should be estimated from the available experimental data, the $P_{>RL}$ values have to be evaluated by means of the corresponding Beta distributions following the approach suggested by Lieberman and Resnikoff (11) and Murphy and Organo (12):

$$P_{RL} = 1 - \int_0^{U_{RL}} \frac{\Gamma(N-2)}{\Gamma\left(\frac{N}{2}-1\right)\Gamma\left(\frac{N}{2}-1\right)} z^{N/2^{-2}} (1-z)^{N/2^{-2}}\,dz$$

where U_{RL} is the upper integration extreme for the variable z corresponding to the given Reference Level.

Material and methods

As no common rules were defined at national level for the mapping procedures, each Region has developed its own approach, based on different assumptions and

Citation: Journal of the European Radon Association 2022, 3: 7719 http://dx.doi.org/10.35815/radon.v3.7719

methodology. The mapping methodology in Piedmont was not developed following an *a priori* theoretical framework clearly established in advance: it was rather a process of adaption to the conditions that were faced. Piedmont Region is a quite large Italian region, with 25,400 km^2 wide and about 4,500,000 inhabitants and 1,181 municipalities. In Piedmont, the municipality, the smallest Italian administrative district, was chosen as the basic sampling unit. However, this choice, very reasonable from the 'political' point of view, was in practice very challenging: the very high number of municipalities, 1,181, actually prevented from performing experimental surveys in each unit based on direct radon measurements; too large would be the number of required measurements and too complicated and costly the management of such campaign. On the other hand, a substantial reduction of the number of sampling units would have brought to an unacceptable loss of details, leading to an almost useless map. In the end, in spite of their high number, the municipalities were taken as basic sampling units by a 'political' reason: the municipality is the smaller administrative unit in Italy, where the prevention policies can effectively be implemented.

While several different technical approaches for mapping are possible, they can be all grouped in two general broad categories:

1. Experimental approach: direct radon measurements of a representative sample of dwellings of the indoor radon activity concentration in any given sampling units.
2. Calculation approach (based on geo-lithological knowledge): evaluation of the 'radon potential' from the geological characteristic of soils and rocks.

In principle, a pure experimental approach should be considered preferable, as the real predictability of the radon activity concentration in buildings from geo-lithological data alone is questionable. Although several different geo-lithological methodologies were proposed (13–16), no complete and generally accepted theories are available at the moment. By contrast, the experimental approach obviously requires a huge number of data, thus resulting in a much more expensive and complicated endeavor. Therefore, in order to reduce the number of the radon experimental measurements to a more manageable amount, a 'mixed approach' was proposed:

1. experimental local surveys in a limited number of selected municipalities (annual measurements) and
2. development of a new radio-geo-lithological classification with homogeneous radon exhalation characteristics, allowing the estimation of the radon concentration values in those municipalities where no experimental measurements are available or their numbers are insufficient.

This approach, combining together two methodologies, the direct radon experimental measurements in dwellings and the considerations based on the underlying geo-lithological characteristics of the sampling units, needs the development of a new classification of the geo-lithological units based on the measurements of the uranium activity concentrations in the rocks by means of γ spectrometry analyses.

We have called this mapping strategy a radio-geo-lithological approach, as the geological units relevant for radon mapping were defined considering not only the official standard geological chart but also the radiometric information coming from a huge experimental work, allowing the radiometric characterization of the most important rocks (geo-lithological units) of Piedmont: more than 440 γ spectrometry measurements with hyperpure germanium detectors (HPGe) were performed (17, 18).

Different classes of lithologies, identified by congruent radionuclide concentrations, are characterized not only by homogeneity of broadly defined rock types but also by common genetic processes. In the Western Alpine region, Cenozoic intrusive rocks with upper crustal contamination and late Paleozoic acid igneous rocks show highest concentrations of natural radionuclides, while mafic and ultramafic rocks of oceanic origin and calcareous Mesozoic rocks show the lowest. Radionuclides' concentrations in detrital rocks and sediments reflect their petrographic compositions, allowing a differentiation of Quaternary glacial, fluvioglacial, and fluvial sediments correlated with radionuclide content and grain size in source rocks within different erosional catchments.

Being operated in this way, it was possible to reduce the initial huge number of units of the geo-lithological map of Piedmont (19) (1:250,000, with more than 200 units, Fig. 2) to the more manageable size of 37 units.

The radon mapping strategy we followed are summarized in five steps, which are as follows:

1. Selection from the database of all the available experimental indoor radon measurements of the data suitable for radon mapping.
2. Normalization of the data and georeferencing.
3. Definition of 37 radio-geo-lithological units.
4. Evaluation of the corresponding radio-geo-lithological indoor radon averages and distributions for each radio-geo-lithological unit using the geo-referenced experimental data.
5. Final model calculation: the average indoor radon concentration in each municipality (considered as the basic sampling unit) is evaluated by means of a proper weighted mean of the radio-geo-lithological means of the units occurring in the municipality. The

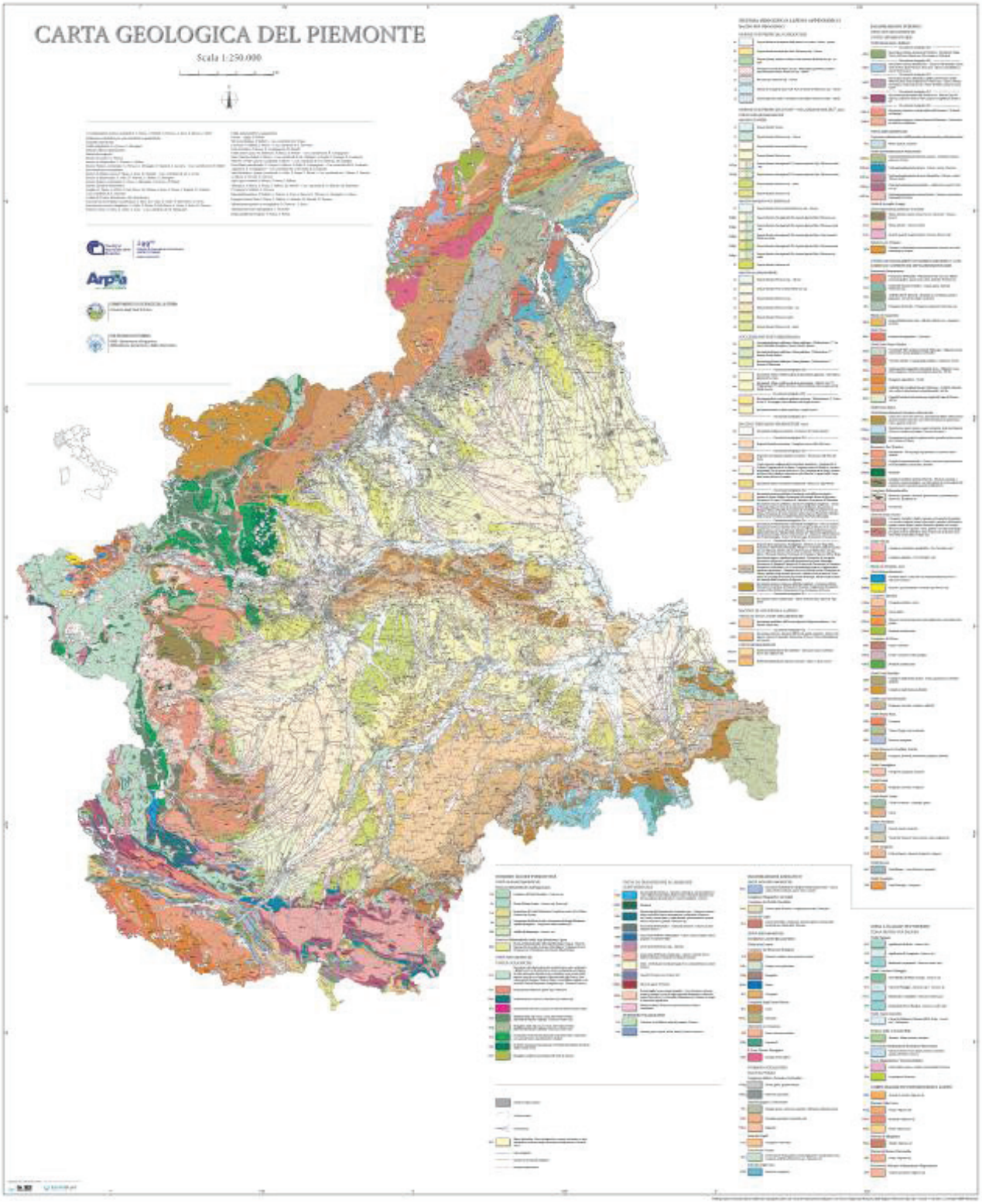

Fig. 2. Piedmont geological map 1:250,000, characterized by more than 200 geo-lithological units.

Citation: Journal of the European Radon Association 2022, **3**: 7719 http://dx.doi.org/10.35815/radon.v3.7719

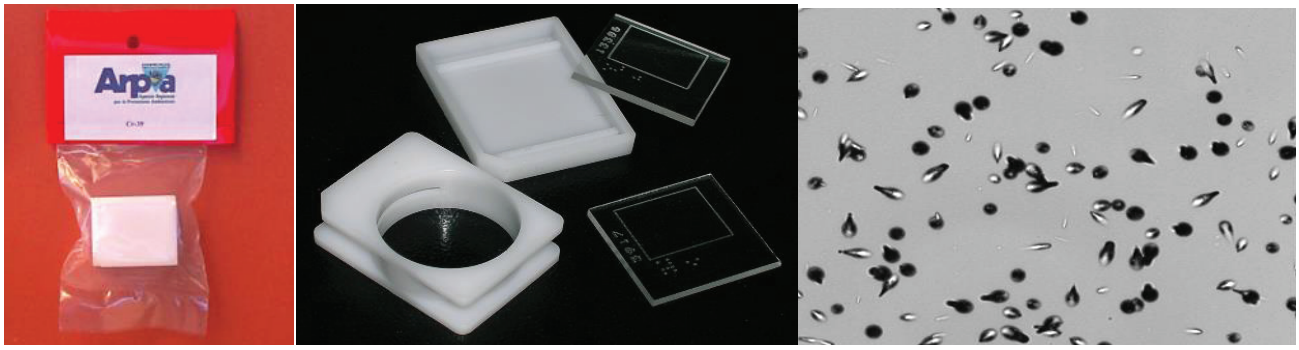

Fig. 3. From left to right: the dosemeter with its radon permeable polyethylene bag, the conductive holder (white) with the CR-39 detectors, and the nuclear α tracks etched at the microscope.

corresponding log-normal distributions are defined as well.

Selection of the experimental data

The measurement considered suitable to be used for the radon mapping shall meet these requirements:

1. annual averaged measurements (usually obtained from two semestral measurements) and
2. performed by means of dosemeters equipped with nuclear track etch a detectors.

The device used in most of our surveys had the following technical characteristics: it contains one or two CR-39 detectors, the holder was made with conductive plastic, and the a detectors were put in thin radon-permeable polyethylene bag (see Fig. 3) (20).

The database used for the radon mapping consisted of 4,389 measurements performed in different types of buildings: 62% dwellings, 31% schools, and 7% other workplaces. All the measurement points were chosen randomly within each sampling unit (municipality). In order to reduce the heterogeneity of sample, the data need to be normalized.

Normalization

Data were subjected to different normalization processes. The most important one was the ground floor normalization. Ground floor indoor radon concentration is recognized as a good indicator for radon mapping purposes also by the law 1 as its value is usually strongly correlated to the soil radon flux and entry rate. However, as a quite high number of the measurements in our database, being randomly chosen, were referred to different floors, in order to put all data together, thus expanding the available dataset, they need to be normalized to ground floor. The ground floor normalization was performed according to the following scheme.

1. Article 11 of the 101/2020 Legislative Decree.

The first assumption was the log-normality for the activity concentration distributions $f(C_X)$ at any given X floor:

$$f(C_X) = \frac{1}{\sqrt{2ps_X}} \frac{e^{-(\ln(C_X)-m_X)^2}}{C_X} \quad (2)$$

The second assumption was a linear relationship between the values at any given floor X and ground floor ones: $C_X = k_X \cdot C_{GF}$. If this is the case, a robust evaluation of the k_X proportional factors can be obtained by simply calculating the ratios of the corresponding geometric means, which is as follows:

$$k_X = \frac{e^{\mu_X}}{e^{\mu_{GF}}} \quad (3)$$

that can be put also in the equivalent form: $\mu_X = \ln k_X + \mu_{GF}$. If this holds, the Geometric Standard Deviation (GSD) of all the distributions is equal, irrespectively from the considered floor $\sigma_x = \sigma_{GF}$.

This seemingly strong assumption is supported by experimental evidence as it was tested on a randomly chosen dwelling sample (more than 400 data) representative of all the Piedmont housing stock (9). In Fig. 4, the results of the normalization procedure are reported: the log-normal function was obtained normalizing to ground floor; all the other data are represented by a solid line, which is very close to the 'true' ground floor distribution (dashed line).

Definition of the radio-geo-lithological units

This was the most difficult and challenging issue, being at the inner core of our approach. We started from a very complicated geological map with more than 200 geological units that should be reduced to a more reasonable number without losing meaningfulness and predictive effectiveness. In the end, 37 units were individuated (see Fig. 5), following geo-lithological considerations

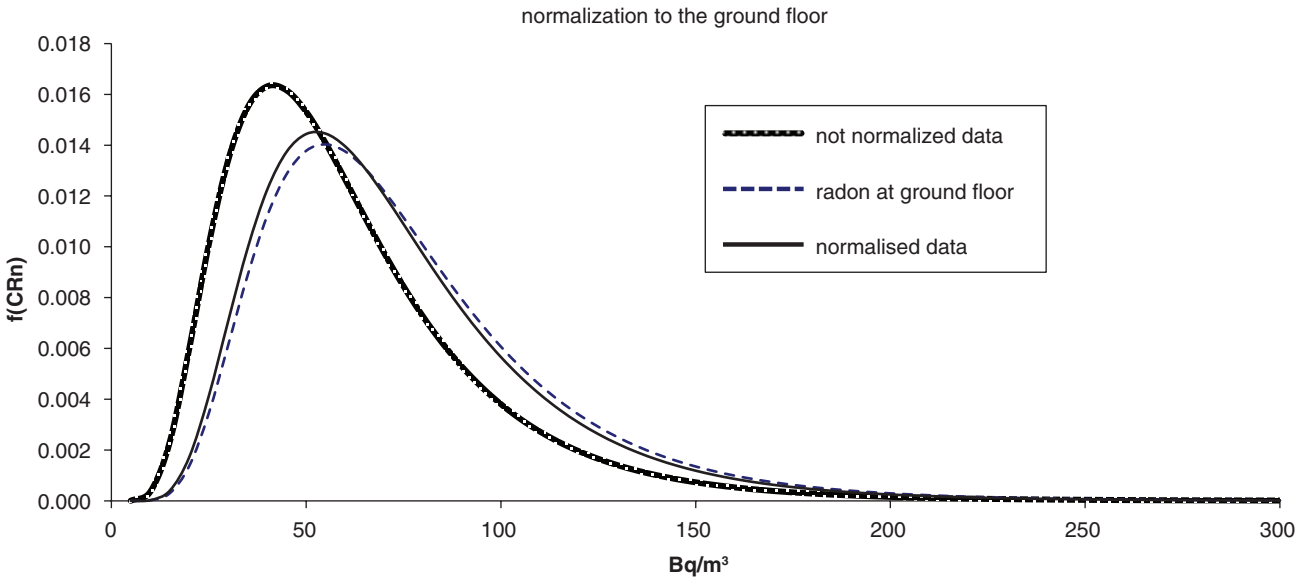

Fig. 4. Normalized data (solid line), ground floor data (dashed line), and not normalized data.

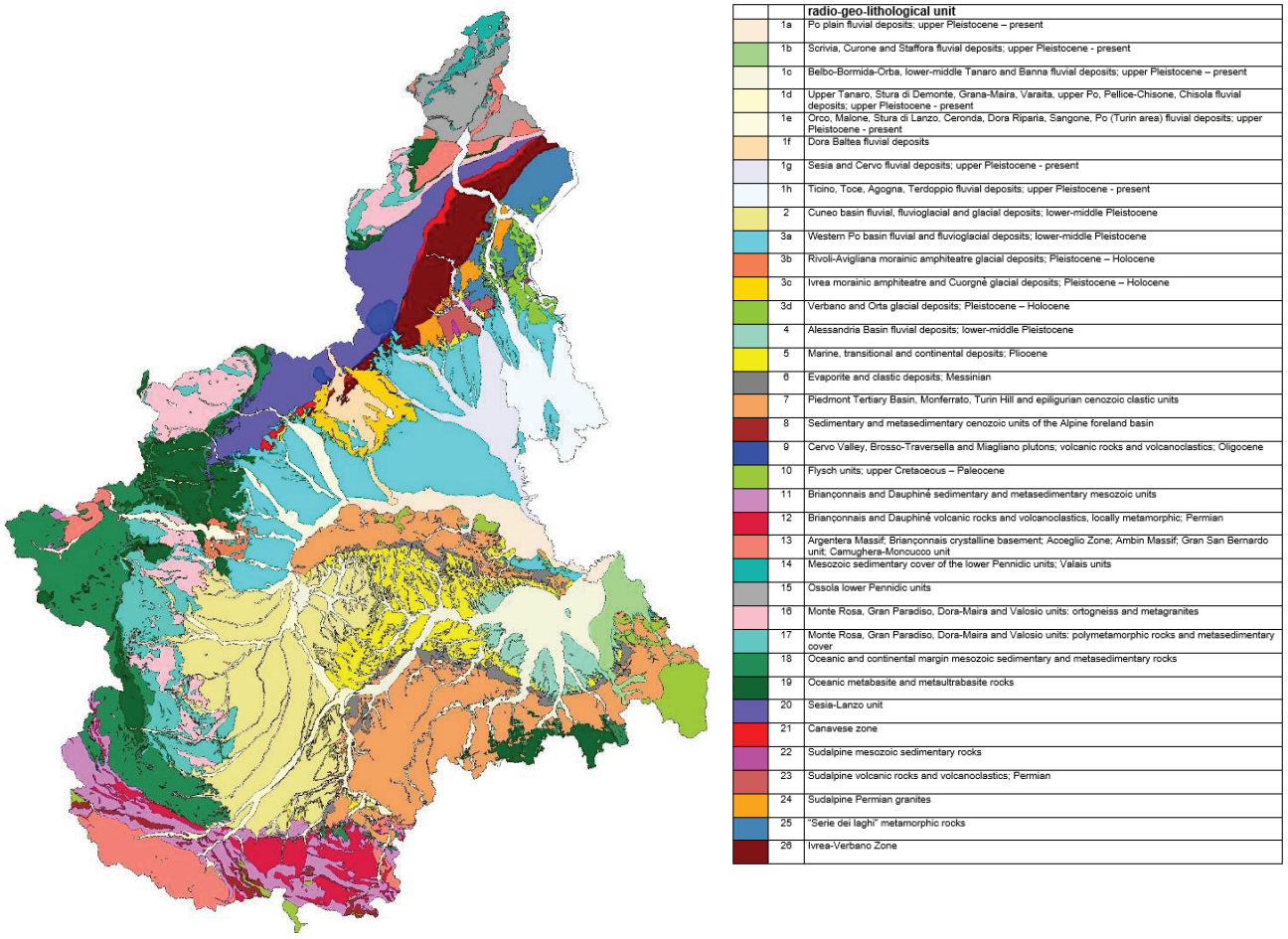

Fig. 5. The 37 different radio-geo-lithological units identified in Piedmont Region.

Citation: Journal of the European Radon Association 2022, **3**: 7719 http://dx.doi.org/10.35815/radon.v3.7719

combined with radiometric information obtained by means of a comprehensive radioactive characterization of the soils and lithologies of Piedmont: actually, more than 440 rock and soil samples gathered all over the Region were measured by means of HPGe γ spectrometry detectors during an extensive campaign that lasted more than 2 years (18). A very similar approach was applied and proved consistent also with the calculation of the terrestrial gamma dose rate in a recent published work (European Atlas of Natural Radiation, pag. 106 (21)). The results of this campaign are summarized in Table 1, where the typical ^{238}U concentrations of the Piedmont's geo-lithologies are shown together with the corresponding radon data. A scatter plot of the radon and the corresponding ^{238}U data are shown as well in Fig. 6.

Calculations of a radio-geo-lithological averages and log-normal distributions

The next step was the calculation of the radio-geo-lithological averages and the log-normal distributions for each unit. To this purpose, all the georeferenced and normalized experimental radon data were superimposed to the radio-geo-lithological map (Fig. 7).

Although no sampling strategy was, of course, possible in order to populate adequately all the radio-geo-lithological units because they were defined after the conclusion of the measurement representative campaigns, it was, however, possible to give a reasonable estimate of the radio-geo-lithological means and of the corresponding parameters μ and σ, characterizing the related log-normal distributions for every generic k radio-geo-lithological unit. In Table 1, the number of experimental data (indoor radon activity concentration) available for each radio-geo-lithological unit and the estimated statistical parameters together with the corresponding ^{238}U concentrations are shown.

Final model calculations

The model not only allows the estimation of the average indoor radon concentration in each sampling unit (municipality) but, taking advantage of the associated log-normal distributions, also permits the evaluation of other important indicators, such as, for example, the percentage of dwellings exceeding any given radon level. The mean value of the radon activity concentration MC_j in each sampling unit j is calculated by means of the following well-known formula: , where μ_j is the weighted mean of the radio-geo-lithological μ_{Lk} of the units occurring in the built areas present in each municipality[2] as follows:

$$\mu_j = \sum_{k=1}^{P} \frac{AL_k \cap AC_j}{AC_j} \times \mu_{Lk}$$

where the weights $\frac{AL_k \cap AC_j}{AC_j}$ are given by the intersection of the radio-geo-lithological area AL_k with the municipality area AC_j over the AC_j itself; the upper limit P in the summation represents the number of radio-geo-lithological units occurring in the built areas of the municipality.

In this approach, a key factor is played by the σ value, that is by the GSD of the log-normal distributions ($GSD = e^{\sigma}$). In principle, each unit should have its own *GSD*, in order to assign to each municipality its own log-normal distribution. However, due to the relatively limited number of experimental data available at the municipality level, we assumed an unique value for all the *GSDs* of the municipalities of the Region ($GSD = 1.74$), following a common approach firstly proposed by Price et al. in 1997 in a very similar context (22): Price and co-workers observed that the values of the *GSDs* experimentally evaluated in different units strongly depend on the sample size and seem to converge to an unique value as the sample size increases. The assumed value was, therefore, calculated considering the asymptotic value of the *GSDs*, obtained for a great number of experimental data (see Fig. 8).

Similar calculations were performed considering as sampling units the 37 radio-geo-lithological units and gave a slightly greater result ($GSD = 1.85$): this was the value adopted for the calculation in those municipalities for which the radon levels had to be estimated by means of equation (5). The problem of the choice of the most adequate *GSD* is still an open issue: in principle, it should be better to assign its own values, experimentally evaluated, to each municipality. However, the solution proposed seems to be adequate as a first approximation, allowing a comprehensive estimation of radon concentration in the whole Region at the municipality level. Moreover, the adopted scheme makes it possible to update the map in a quite simple way as new experimental data become available.

The model was then validated comparing the experimental average municipality values (when available) to the estimated ones, avoiding any self-correlation bias.[3] In order to increase the reliability, only those municipalities where more than 10 experimental measurements were available have been considered. The validation was, thus, performed considering 120 couples of experimental-estimates data. An average value very close to 1 for the ratio experimental/predicted values (0.96; $R^2 = 0.86$) was found.

2. In our work we have considered only the built areas rather than the total municipality areas, in order to give a more realistic description. If no information about the built areas were available the total municipality areas were considered as a first approximation.

3. Excluding the experimental data gathered in each municipality from the dataset used for the calculation of radio-geo-lithological means

Table 1. The radio-geo-lithological unit of Piedmont

Leg.	Radio-geo-lithological unit	^{222}Rn Data	^{222}Rn Bq/m^3 Mean	^{222}Rn Bq/m^3 Median	μ	σ	^{238}U Data	^{238}U (Bq/kg) Min–Max–Median
1a	Po plain fluvial deposits; upper Pleistocene – present	165	74	63	4.15	0.52	8	31–136–39
1b	Scrivia, Curone, and Staffora fluvial deposits; upper Pleistocene – present	49	81	73	4.30	0.42	4	29–51–31
1c	Belbo-Bormida-Orba, lower-middle Tanaro, and Banna fluvial deposits; upper Pleistocene – present	194	77	69	4.23	0.44	20	10–76–26
1d	Upper Tanaro, Stura di Demonte, Grana-Maira, Varaita, upper Po, Pellice-Chisone, and Chisola fluvial deposits; upper Pleistocene – present	262	163	116	4.75	0.79	9	4–48–28
1e	Orco, Malone, Stura di Lanzo, Ceronda, Dora Riparia, Sangone, and Po (Turin area) fluvial deposits; upper Pleistocene – present	184	79	67	4.20	0.55	8	1–62–31
1f	Dora Baltea fluvial deposits	58	73	63	4.15	0.55	1	41–41–41
1g	Sesia fluvial deposits; upper Pleistocene – present	87	94	82	4.41	0.48	7	21–91–36
1g3a	Cervo fluvial deposits	68	183	129	4.86	0.76	1	25–25–25
1h	Ticino, Toce, Agogna, and Terdoppio fluvial deposits; upper Pleistocene – present	174	115	93	4.54	0.62	2	45–59–52
2	Cuneo basin fluvial, fluvioglacial, and glacial deposits; lower-middle Pleistocene	572	141	98	4.58	0.78	18	7–133–39
3a	Western Po basin fluvial and fluvioglacial deposits; lower-middle Pleistocene	1,028	77	59	4.09	0.64	29	17–140–58
3b	Rivoli-Avigliana morainic amphiteatre glacial deposits; Pleistocene – Holocene	28	97	85	4.44	0.54	1	27–27–27
3c	Ivrea morainic amphiteatre and Cuorgnè glacial deposits; Pleistocene – Holocene	75	66	56	4.02	0.54	13	15–71–39
3d	Verbano and Orta glacial deposits; Pleistocene – Holocene	78	113	89	4.49	0.62	1	39–39–39
4	Alessandria Basin fluvial deposits; lower-middle Pleistocene	44	73	62	4.13	0.54	9	13–94–52
5	Marine, transitional, and continental deposits; Pliocene	150	90	72	4.28	0.57	8	26–102–47
6	Evaporite and clastic deposits; Messinian	16	84	72	4.28	0.52	6	9–34–20
7	Piedmont Tertiary Basin, Monferrato, Turin Hill, and epiligurian cenozoic clastic units	129	78	68	4.22	0.48	47	12–81–29
8	Sedimentary and metasedimentary cenozoic units of the Alpine foreland basin	45	97	78	4.36	0.71	1	24–24–24
9	Cervo Valley, Brosso-Traversella, and Miagliano plutons; volcanic rocks and volcanoclastics; Oligocene	117	537	337	5.82	1.07	10	40–501–139
10	Flysch units; upper Cretaceous – Paleocene	46	64	61	4.11	0.42	8	19–60–39
11	Briançonnais and Dauphiné sedimentary and metasedimentary mesozoic units	60	119	88	4.48	0.72	13	2–165–32
12	Briançonnais and Dauphiné volcanic rocks and volcanoclastics, locally metamorphic; Permian	62	122	90	4.50	0.78	8	6–58–37
13	Argentera Massif, Briançonnais crystalline basement, Acceglio Zone, Ambin Massif, Gran San Bernardo unit, and Camughera-Moncucco unit	26	121	95	4.55	0.69	8	3–97–26

Citation: Journal of the European Radon Association 2022, **3**: 7719 http://dx.doi.org/10.35815/radon.v3.7719

Table 1. (continued) The radio-geo-lithological unit of Piedmont.

Leg.	Radio-geo-lithological unit	^{222}Rn Data	^{222}Rn Bq/m^3 Mean	^{222}Rn Bq/m^3 Median	μ	σ	^{238}U Data	^{238}U (Bq/kg) Min–Max–Median
14	Mesozoic sedimentary cover of the lower Pennidic units; Valais units	24	99	77	4.35	1.04	5	30–78–49
15	Ossola lower Pennidic units	34	100	82	4.40	0.62	12	4–106–62
16	Monte Rosa, Gran Paradiso, Dora-Maira, and Valosio units: ortogneiss and metagranites	62	187	127	4.85	0.82	16	4–96–58
17	Monte Rosa, Gran Paradiso, Dora-Maira, and Valosio units: polymetamorphic rocks and metasedimentary cover	24	134	93	4.53	0.79	11	10–115–43
18	Oceanic and continental margin mesozoic sedimentary and metasedimentary rocks	61	87	75	4.32	0.54	26	1–81–26
19	Oceanic metabasite and metaultrabasite rocks	40	76	60	4.10	0.83	17	0–59–17
20	Sesia-Lanzo unit	126	84	66	4.19	0.65	14	2–76–42
21	Canavese zone	24	76	58	4.06	0.73	4	17–60–49
22	Sudalpine mesozoic sedimentary rocks	25	126	112	4.71	0.52	1	11–11–11
23	Sudalpine volcanic rocks and volcanoclastics; Permian	17	83	80	4.39	0.32	5	43–141–73
24	Sudalpine Permian granites	45	116	100	4.60	0.52	3	22–69–53
25	'Serie dei laghi' metamorphic rocks	113	134	91	4.52	0.79	6	26–79–38
26	Ivrea-Verbano Zone	108	70	59	4.08	0.56	23	0–163–2

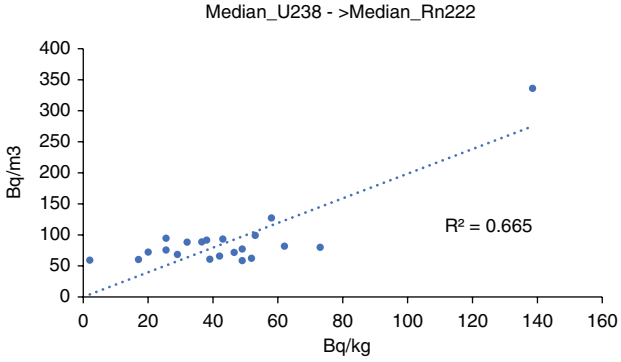

Fig. 6. ^{222}Rn/^{238}U scatter plot of the radio-geo-lithologies (no fluvial deposits).

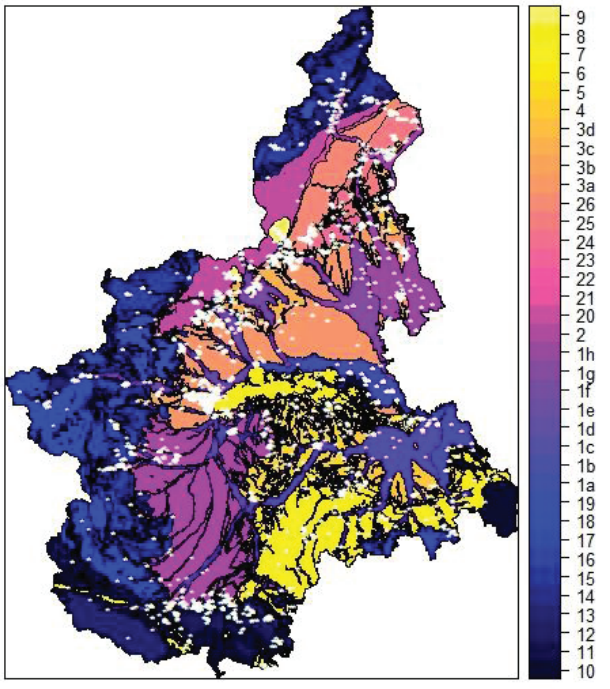

Fig. 7. The radio-geo-lithological map of Piedmont with the radon measurements superimposed (white dots).

Results and discussion

In Figs. 9 and 10, the radon maps of Piedmont calculated following the procedures described in previous section are shown.

From these maps, some very interesting information concerning the radon exposure in dwellings at regional level and for each municipality as well can be obtained. An average activity concentration of 74 Bq/m^3 was found (weighted mean of all the available data), a value somewhat greater than that obtained about 30 years ago (69 Bq/m^3), in the first Italian National Campaign (1990–1991). The observed difference could be explained by two factors: a possible underestimation during the National Campaign due to the under-sampling of some of the most radon affected areas and an effect of the implementation of the recent energy saving policies that,

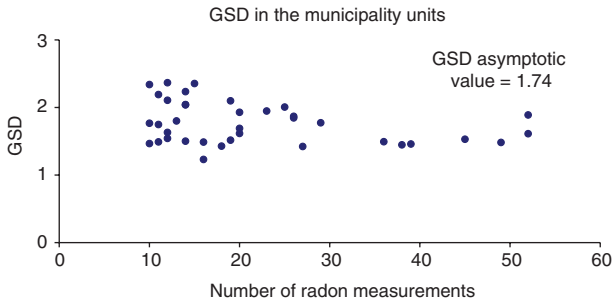

Fig. 8. The experimentally evaluated GSD tends to an asymptotic value as the number of measurements increases (22).

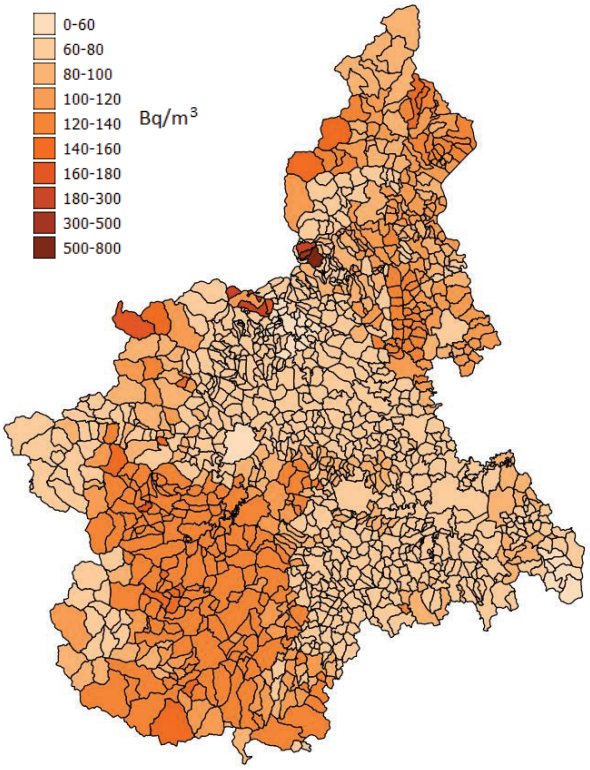

Fig. 9. Map showing the radon mean values for all the municipalities of Piedmont, the average regional value being 74 Bq/m^3.

in many cases, lead to a substantial reduction of the building ventilation rate.

The model allowed also the identification of the RPAs, defined accordingly to the provisions established by the Italian law (every municipality where the ground floor activity concentration exceeds 300 Bq/m^3 in more than 15% of the buildings).

According to this criterion (see Fig. 10), about 10 municipalities, mainly located in the alpine and pre-alpine area, should be classified as RPAs.

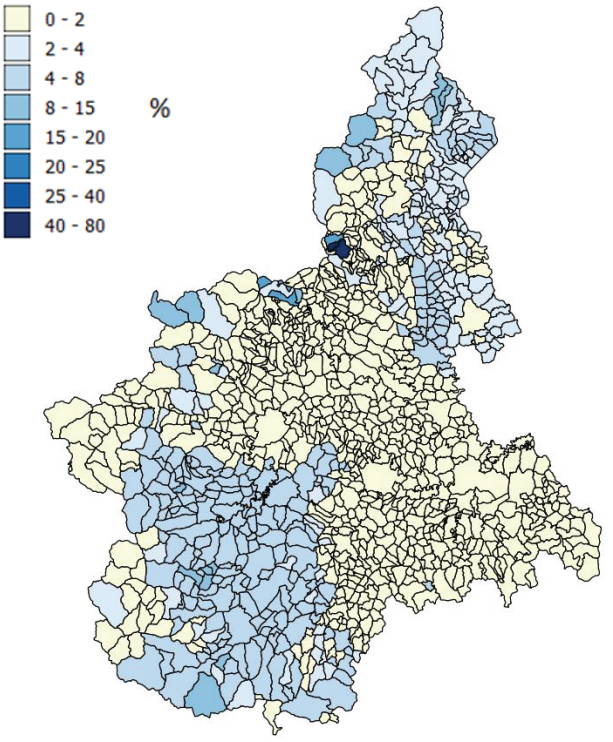

Fig. 10. Percentage of dwellings exceeding 300 Bq/m^3 (the Italian Reference Level) for both homes and workplaces (Legislative Decree 101/2020 implementing the Euratom Directive 59/2013) evaluated following the Andersen approach (see Ref. 12).

Conclusions

A radio-geo-lithological model was developed, allowing a comprehensive radon mapping of Piedmont, considering, as basic sampling units, all 1,181 municipalities in which Piedmont is subdivided. The proposed method, characterizing each municipality by its own log-normal distribution, allows a quite detailed estimation of the exposure to radon of the population of Piedmont, thus permitting the implementation of effective policies supporting a medium long-term reduction of the health impact of radon all over the Region. The structure of the adopted model is quite flexible, easily allowing a progressive update of the maps as new experimental data become available.

Conflict of interest and funding

The authors have not received any funding or benefits from industry or elsewhere to conduct this study.

References

1. COUNCIL DIRECTIVE 2013/59/EURATOM of 5 December 2013, Official Journal of the European Union 17 January 2014, L13/1.
2. Bochicchio F, Campos Venuti G, Nuccetelli C, Piermattei S, Risica S, Tommasino L, et al. Results of the representative

Citation: Journal of the European Radon Association 2022, 3: 7719 http://dx.doi.org/10.35815/radon.v3.7719

Italian national survey on radon indoors. Health Phis 1996; 71(5): 741–48. doi: 10.1097/00004032-199611000-00016
3. Bochicchio F, Campos Venuti G, Nuccetelli C, Piermattei S, Risica S, Tommasino L, et al. Annual average and seasonal variations of residential radon concentration for all the Italian Regions. Radiat Meas 2005; 40: 686–94. doi: 10.1016/j.radmeas.2004.12.023
4. Magnoni M, and Tofani S. Valutazioni della concentrazione di radon nelle abitazioni del Piemonte (in Italian). Proceeding of the Conference: La qualità dell'aria negli ambienti di vita. ENEA Publication; Pisa – Italy, 28–29 October 1992.
5. Bochicchio F, Campos Venuti G, Piermattei S, Torri G, Nuccetelli C, Risica S, et al. Areas with high radon levels in Italy. Proceedings of the Conference: Radon in the Living Environment, Athens – Greece, 19–23 April 1999.
6. ISS-ANPA. Indagine nazionale sulla radioattività naturale nelle abitazioni, (in Italian). Proceeding of the Conference ISTISAN Congressi 34; 1994.
7. Magnoni M, and S. Tofani. Indoor radon measurements in anomalous sites of Piedmont, Italy. Radiat Protect Dosimetry 1994; 56: 327–9. doi: 10.1093/oxfordjournals.rpd.a082481
8. ARPA Piemonte. La mappatura del radon in Piemonte. 2009 (in Italian). Available from: https://www.arpa.piemonte.it/pubblicazioni-2/pubblicazioni-anno-2009/la-mappatura-del-radon-in-piemonte [cited 28 June 2021].
9. Chiaberto E, Magnoni M, Serena E, Procopio S, Prandstatter A, Righino F. Radon potential mapping in Piemonte (North-West Italy): An experimental approach. Eur Phys J. Web of Conf 2012; 24: 06003.
10. DECRETO LEGISLATIVO 31 luglio 2020, n. 101 (Attuazione Direttiva 2013/59/Euratom), Gazzetta Ufficiale della Repubblica Italiana, Serie Generale n.201 del 12-08-2020 – Suppl. Ordinario n. 29.
11. Lieberman GJ, Resnikoff GJ. Sampling plans for inspections by variables. J Am Stat Assoc 1995; 50(270): 457–516. Available from: http://www.jstor.org/stable/2280972 [cited 4 April 2014].
12. Murphy P, Organo C. A comparative study of lognormal, gamma and beta modeling in radon mapping with recommendations regarding bias, sample sizes and the treatment of the outliers. J Radiol Protect 2008; 28: 293–302. doi: 10.1088/0952-4746/28/3/001
13. Miles J. Development of maps of radon-prone areas using radon measurements in houses. Oxford: Elsevier Science; 1998.
14. Bossew P, Dubois G, Tollefsen T. Investigations on indoor Radon in Austria, part 2: geological classes as categorical external drift for spatial modelling of the Radon potential. J Environ Radioact 2008: 99(1); 81–97. doi: 10.1016/j.jenvrad.2007.06.013
15. Miles J, Appleton D. Mapping variation in radon potential both between and within geological units. J Radiat Prot 2005; 25(3); 257. doi: 10.1088/0952-4746/25/3/003
16. Gundersen LCS, Schumann RR. Mapping the radon potential of the United States: examples from the Appalachians. Environ Int 1996; 22: S829–37. doi: 10.1016/S0160-4120(96)00190-0
17. Magnoni M, Bertino S, Tripodi R, Bellotto B. La misura dell'^{238}U mediante spettrometria gamma in matrici ambientali (in Italian). Proceedings Convegno Nazionale AIRP-Pisa, 4–6 June 2008.
18. Falletti P, Chiaberto E, Serena E, Prandstatter A, Tripodi R, Magnoni M, et al. Radionuclidi naturali nelle rocce del Piemonte: verso la definizione del potenziale geogenico radon (in Italian). Proceedings of the VI Physical Agents National Congress, Alessandria, 6–8 June 2016.
19. Piana F, Falletti P, Fioraso G, Mosca P, Irace A, d'Atri A. Carta geologica del Piemonte alla scala 1:250.000, ARPA Piemonte; 2012.
20. Tommasino L, Cherouati D.E, Seidel J.L, Monnin M. Plastic-bag sampler for passive radon monitoring. Nuclear Tracks 1986; 12(1–6): 681–4. doi: 10.1016/1359-0189(86)90678-3
21. Cinelli G, De Cort M, Tollefsen T. European atlas of natural radiation. Publication Office of the European Union, Luxembourg; 2019. doi: 10.2760/520053
22. Price PN. Predictions and maps of country mean indoor radon concentrations in the mid-Atlantic states. Health Phys 1997; 72(6): 893–906.

***Mauro Magnoni**
Via Jervis, 30 – 10015
Ivrea, TO, Italy
Email: mauro.magnoni@arpa.piemonte.it